Applied Catalysis A: General 478 (2014) 267–274

Contents lists available at ScienceDirect

Applied Catalysis A: General

journal homepage: www.elsevier.com/locate/apcata

An efficient eco-sustainable oxidative desulfurization process using μ-oxo-bridged Fe(III) complex of *meso*-tetrakis(pentafluorophenyl)porphyrin

António Aguiar, Susana Ribeiro, André M.N. Silva, Luís Cunha-Silva, Baltazar de Castro, Ana M.G. Silva, Salete S. Balula*

REQUIMTE, Departamento de Química e Bioquímica, Faculdade de Ciências, Universidade do Porto, 4169-007 Porto, Portugal

ARTICLE INFO

Article history:
Received 20 December 2013
Received in revised form 26 March 2014
Accepted 1 April 2014
Available online 13 April 2014

Keywords:
μ-Oxodimeric iron(III) porphyrin
Hydrogen peroxide
Oxidative desulfurization
Homogeneous catalysis
Benzothiophene derivatives

ABSTRACT

The present work is the first report of using a Fe^{III} dimeric porphyrin as an active and efficient catalyst for the oxidative desulfurization of a multicomponent oil formed by the most refractory sulfur compounds in fuels (dibenzothiophene, DBT, 1-benzothiophene, 1-BT, and 4,6-dimethyldibenzothiophene, 4,6-DMDBT), using the biphasic system model oil/extraction solvent. The binuclear μ-oxodiiron(III) complex of *meso*-tetrakis(pentafluorophenyl)porphyrin μ-O(FeTPFPP)$_2$, was synthesized and characterized by UV/Vis spectroscopy, mass spectrometry and single-crystal X-ray diffraction. μ-O(FeTPFPP)$_2$ was shown to achieve a complete desulfurization after 2 h when acetonitrile and methanol were used as extraction solvents, in the presence of a residual amount of H_2O_2 as oxidant, at room temperature. The catalytic efficiency of the porphyrin was evaluated for each refractory sulfur compound following the order 1-BT > DBT > 4,6-DMDBT. Surprisingly, the porphyrin presents a remarkable catalytic performance for the desulfurization of 1-BT when compared with other catalysts already reported in the literature. Furthermore, the extracting phase containing the porphyrin could be reused in consecutive desulfurization cycles.

1. Introduction

Current fuel regulations that limit sulfur content to ultra low levels have been crucial in minimizing the negative health and environmental effects associated with air pollution and acid rains caused by the sulfur oxides (SOx) formed during combustion of transportation fuels. In the near future, zero-emission is expected worldwide. Therefore, an increase attention has been given to create novel and efficient desulfurization technologies [1,2]. Hydrodesulfurization (HDS) is the conventional process most widely used in petroleum refineries to reduce sulfur contents in fuels. This method converts organic sulfur into hydrogen sulfide and it is highly efficient in removing thiols, sulfides and disulfides, but it is less successful for refractory sulfur containing compounds, such as thiophene and benzothiophene derivatives [3,4]. Apart from the efficiency of the HDS, this technology has some technical and economic problems, such as severe operating conditions (hydrogen pressure greater than 2 MPa and temperature above 300 °C) and high operation/equipment cost [5]. Therefore, it is desirable to develop alternative and also supplementary approaches to the actual HDS method to produce ultra deep desulfurization for the production of clean transportation fuels. Various alternatives have been proposed in the literature including biodesulfurization, alkylation desulfurization, selective adsorption and oxidative desulfurization (ODS) [4,6]. Among these methods, the ODS process is considered to be one of the most promising alternatives, since it avoids the use of hydrogen and can be conducted under ambient conditions at atmospheric pressure [4,7]. Furthermore, the ODS technology has shown to be highly efficient mainly for the extraction of the most refractory sulfur compounds such as the dibenzothiophene (DBT) and its derivatives [4,5,7–9]. In fact, the ODS process combines two main steps: one is based on the catalytic oxidation of sulfur compounds to their corresponding sulfoxides and sulfones in the presence of an oxidant, and the other step consists in the extraction of the oxidized products using a suitable extraction solvent or an absorbing material [8]. Hydrogen peroxide has been largely used as the oxidant in the ODS technology, mainly because it is an eco-sustainable

---

* Corresponding authors. Tel.: +351 220402576; fax: +351 220402659.
E-mail addresses: ana.silva@fc.up.pt (A.M.G. Silva), sbalula@fc.up.pt (S.S. Balula).

http://dx.doi.org/10.1016/j.apcata.2014.04.002

oxidant. Furthermore, the by-products of the ODS process, sulfones and sulfoxides, are potential sources of organic intermediates and bioactive compounds for pharmaceutical applications [10,11].

It is known that metalloporphyrins, in particular the highly halogenated complexes of *meso*-2,6-dichlorophenyl and *meso*-pentakis(pentafluorophenyl)porphyrinatoiron(III), are very effective on different catalytic systems [12–16]. However, the application of metalloporphyrins in the oxidative desulfurization processes is practically unexplored. To our knowledge, only one work has been published using an iron porphyrin as catalyst for the oxidation of a model oil containing DBT or 4,6-dimethyldibenzothiophene (4,6-DMDBT) in the presence of molecular oxygen at 120 °C; however, in this study the extraction of the oxidized sulfur compounds from the model oil was not performed [17]. Neves et al. [18] have recently reported the oxidation of various organosulfur compounds catalyzed by manganese porphyrins in the presence of ammonium acetate as co-catalyst, using hydrogen peroxide as oxidant and acetonitrile or hexane as solvents. In the same year, Rezaeifard et al. [19] have also published the application of manganese porphyrins as catalyst for the oxidation of various aryl sulfides in the presence of different nitrogen donors used as co-catalysts and tetra-n-butylammonium peroxomonosulfate as oxidant.

μ-Oxo-bridged Fe(III) complexes, like μ-O(FeP)$_2$, traditionally named μ-oxodimers, have very peculiar catalytic properties. Investigations over the past decades indicated that μ-oxo-bridged Fe(III) porphyrins have high catalytic activity for the oxidation of 2-methylbutane, cyclohexane and ethylbenzene [20–22]. Moreover, the catalysis of simple μ-oxo dimeric metalloporphyrins for epoxidation of olefins by oxygen have been recently reported [23]. Thus, the synthesis of μ-oxodimers from various analogues of Fe(III) porphyrins and the study of their structures, reactivities and stabilities is currently of considerable interest.

The present work reports for the first time the application of a porphyrin (μ-oxo-bridged Fe(III) porphyrin complex of *meso*-tetrakis(pentafluorophenyl)porphyrin [μ-O(FeTPFPP)$_2$]) as an efficient catalyst for the oxidative desulfurization (ODS) process using a multicomponent oil containing the most representative refractory sulfur compounds in fuels. The ODS process here proposed operates using eco-sustainable conditions (using H_2O_2 as oxidant and no co-catalyst was needed) and it could be reused for several cycles without loss of activity.

2. Experimental

2.1. Materials

Meso-tetrakis(pentafluorophenyl)porphyrin (TPFPP) was prepared by a procedure previously reported [24]. Reagents and solvents used in the preparation of the μ-oxo-bridged Fe(III) porphyrin, namely iron(II) chloride (Aldrich), pyridine (Aldrich) and *N,N*-dimethylformamide (DMF, Aldrich) were used as received without further purification. The reagents used in the catalytic studies, such as dibenzothiophene (DBT, Aldrich), 1-benzothiophene (1-BT, Aldrich), 4,6-dimethyldibenzothiophene (4,6-DMDBT, Aldrich), *n*-octane (VWR), acetonitrile (MeCN, Fisher Chemical), *N,N*-dimethylformamide (DMF, Aldrich), methanol (MeOH, Merck), hydrogen peroxide 30% (Riedel-de-Häen), 1-butyl-3-methylimidazolium hexafluorophosphate (BMIPF$_6$, Aldrich) and 1-butyl-3-methylimidazolium tetrafluoroborate (BMIBF$_4$) were used as received.

2.2. Synthesis of μ-O(FeTPFPP)$_2$

The dimeric porphyrin was synthesized adding pyridine (0.42 mL, 5.20 mmol) and $FeCl_2 \cdot H_2O$ (0.21 g, 0.16 mmol) to a DMF solution of *meso*-tetrakis(pentafluorophenyl)porphyrin (TPFPP) (100 mg, 0.10 mmol) under argon atmosphere. The resulting mixture was refluxed and after one hour, more pyridine (0.42 mL, 5.2 mmol) and $FeCl_2 \cdot H_2O$ (0.21 g, 0.16 mmol) were added to the reaction mixture, and the reflux continued for another hour. The mixture was allowed to cool to room temperature and left in contact with air for 18 h. Then, the solvents of the reaction mixture were evaporated to dryness. The resulting residue was poured into water and extracted three times with dichloromethane. The dichloromethane extract was dried with anhydrous Na_2SO_4 and it was evaporated to dryness to give a solid residue. Then, the residue was recrystallized from dichloromethane/n-hexane.

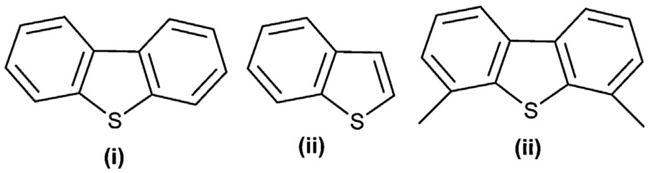

Scheme 1. Chemical structures of the refractory sulfur compounds.

2.3. Catalytic oxidative desulfurization process (ODS)

The oxidative desulfurization studies were performed using model oils previously prepared by dissolution of the refractory sulfur-compounds present in fuels: dibenzothiophene, 1-benzothiophene and 4,6-dimethyldibenzothiophene (i, ii and iii in Scheme 1, respectively), in *n*-octane to form solutions of 500 ppm of sulfur from each substrate. ODS experiments were carried out under air (atmospheric pressure) in a closed borosilicate 5 mL reaction vessel, equipped with a magnetic stirrer. The ODS studies were performed using the biphasic systems with the model oil and an extraction solvent. The desulfurization efficiency of porphyrin μ-O(FeTPFPP)$_2$ was compared using various extraction solvents: acetonitrile, methanol, dimethylformamide, and the ionic liquids (1-butyl-3-methylimidazolium hexafluorophosphate, BMIPF$_6$ and tetrafluoroborate, BMIBF$_4$). In a typical catalytic reaction, 1 μmol of μ-O(FeTPFPP)$_2$ were added to 0.75 mL of the extraction solvent and 0.75 mL of the multicomponent oil was added. This mixture was stirred for 10 min until the initial extraction equilibrium was reached. An aliquot from the upper oil phase was taken. The catalytic reaction was initiated by the addition of the oxidant H_2O_2 (5, 10 and 30 μL). To optimized the amount of oxidant, different S/oxid ratios were performed: 0.75 (H_2O_2 = 5 μL), 0.37 (H_2O_2 = 10 μL) and 0.12 (H_2O_2 = 30 μL). The sulfur content in the model oil was quantified periodically by GC analysis. Tetradecane was used as standard. The most efficient ODS μ-O(FeTPFPP)$_2$ system was reused after each complete desulfurization process by removing the desulfurized oil and adding a fresh oil portion and more oxidant H_2O_2.

2.4. Physical measurements

Electronic absorption spectra were recorded on a Varian Cary 50 Bio spectrophotometer. High resolution electrospray ionisation mass spectra (ESI-MS) were obtained in a Thermo Scientific LTQ-Orbitrap XL mass spectrometer, externally calibrated with a standard kit provided by the manufacturer. Samples were dissolved in methanol and directly infused into the electrospray ion source utilizing the seringe pump in the mass spectrometer at 10 μl min^{-1}. The spectrometer was operated in the positive ionization mode setting the capilary voltage to +3.1 kV, sheath gas flow to 6 and the temperature of the ion transfer capillary to 275 °C. Spectra were recorded for m/z values between 400 and 3500 in the Fourrier Transform (FT) mode with resolution (FWHM) set at 30000. GC-FID was carried out in a Bruker 430-GC to follow the reactions. In

Table 1
Crystal and structure refinement data for the complex [μ-O(FeTPFPP)$_2$].

Formula	$C_{101}H_{46}Cl_2F_{40}Fe_2N_8O$
Mr	2330.06
Crystal morphology	Prism violet
Crystal size/mm	0.25 × 0.10 × 0.09
Crystal system	Tetragonal
Space group	$I4_1/a$
a (Å)	26.3539(19)
b (Å)	26.3539(19)
c (Å)	30.877(3)
$\alpha=\beta=\gamma$ (°)	90
Volume (Å^3)	21445(3)
Z	8
$\rho_{\text{calculated}}$ (g cm^{-3})	1.443
F(0 0 0)	9296
μ (mm^{-})	0.439
θ range (°)	3.70 to 25.68
Index ranges	$-32 \le h \le 32$ $-32 \le k \le 24$ $-37 \le l \le 36$
Reflections collected	62540
Independent reflections	10144 ($R_{\text{int}}=0.0522$)
Final R indices [$I>2\sigma(I)$]	$R_1=0.0628$; $wR_2=0.1767$
Final R indices (all data)	$R_1=0.0971$; $wR_2=0.2074$
Largest diff. peak and hole/e (Å^3)	0.758 and −0.613

both experiments, the hydrogen was the carrier gas (55 cm^3 s^{-1}) and fused silica Supelco capillary columns SPB-5 (30 m × 0.25 mm i.d.; 25 μm film thickness) were used.

2.5. Single-crystal X-ray diffraction

Crystalline material of the complex [μ-O(FeTPFPP)$_2$] was manually harvested, and a suitable single crystal was mounted on a Hampton Research cryo-loop using adequate viscous oil [25]. Diffraction data acquisition was performed on a Bruker X8 Kappa APEX II Charge-Coupled Device (CCD) area-detector diffractometer with the collection controlled by the APEX2 software package [26]: Mo K$_\alpha$ graphite-monochromated radiation, $\lambda=0.71073$ Å; crystal was positioned at 40 mm from the detector and using 90 s of exposure time; temperature of acquisition (180 K) was set up with liquid nitrogen stream by the Oxford Cryosystems Series 700 monitored by the interface Cryopad [27]. Images were processed in the software SAINT+, [28] and the correction of the absorption effects was carried out by multi-scan semi-empirical method implemented in SADABS [29]. The structure was solved by the direct methods implemented in SHELXS-97, [30,31] allowing the immediate identification of some heaviest elements, with the remaining atoms of the structure subsequently located from the difference Fourier maps calculated by successive full-matrix least-squares refinement cycles on F^2 using SHELXL-97 [31,32].

All non-hydrogen atoms of the structure were successfully refined with anisotropic displacement parameters, excepting those of the solvent molecules (hexane and dichloromethane) which were refined only with isotropic parameters. Hydrogen atoms of the porphyrin and solvent molecules were located at their geometrical positions using appropriate *HFIX* instruction in SHELXL (43 for the aromatic, 23 for the–CH$_2$–and 137 for the–CH$_3$ groups), and incorporated in subsequent refinement cycles in riding-motion approximation with isotropic with isotropic thermal displacements parameters (U_{iso}) fixed at 1.2 or 1.5 × U_{eq} of the respective carbon atom.

Information of crystallographic data collection and structure refinement details is summarized in Table 1. Crystallographic data (excluding structure factors) have been deposited with the Cambridge Crystallographic Data Centre as supplementary publication n(CCDC-977858. Copies of the data can be obtained free of charge on application to CCDC, 12 Union Road, Cambridge CB2 2EZ, UK (fax: +44 1223 336033, or online via www.ccdc.cam.ac.uk/data_request/cif or by emailing data_request@ccdc.cam.ac.uk.

3. Results and discussion

3.1. Synthesis and characterization of μ-O(FeTPFPP)$_2$

The complex μ-O(FeTPFPP)$_2$ was synthesized by refluxing a mixture of *meso*-tetrakis(pentafluorophenyl)porphyrin (TPFPP) and iron(II) chloride, in dry DMF in the presence of pyridine. After the refluxing period the reaction mixture was left in contact with air for 18 h. The porphyrin complex [μ-O(FeTPFPP)$_2$] was unequivocally confirmed by the crystal structure. Crystalline material of the complex with quality for single-crystal X-ray diffraction (XRD) analysis was isolated by cautious recrystallization from a mixture of hexane/dichloromethane, and the structure revealed a compound formulated as [μ-O(FeTPFPP)$_2$]·2(C$_6$H$_{12}$)·(CH$_2$Cl$_2$). The crystal structure of the complex was determined in the tetragonal space group $I4_1/a$, with the asymmetric unit containing half of the porphyrin complex {[μ-O(FeTPFPP)$_2$]$_{1/2}$} and two solvent molecules (one hexane and a dichloromethane molecule with partially occupancy of 50%). This structure is identical to that reported previously by Gold et al., being the main differences related with the crystallization solvent molecules [33]. The crystal structure revealed two cationic (FeTPFPP)$^+$ units bridged by a O^{2-} anion, with an angle Fe–O–Fe practically linear [178.4(2)] and leading to a Fe···Fe distance of 3.5456(2) Å (Fig. 1). The crystallographic independent Fe(III) centre (Fe1) shows a slightly distorted square pyramidal coordination geometry, with the base formed by four N-atoms of the pyrrole rings and the O-atom in the apical position: all the Fe1–N distances are considerable close ranging from 2.085(3) to 2.103(3) Å, while Fe1–O1 distance is 1.7730(5) Å, being comparable to that previous observed in related porphyrin complexes (see Table 2 for more details concerning bond distances and angles of the Fe coordination centre) [34–39]. The conformation of the complex (Fig. 1a and b) and its crystalline packing (Fig. 1c) are mainly driven by the steric requirements of the fully fluorinated meso-phenyl groups, originating cavities which are filled by the solvent molecules (hexane and dichloromethane). Furthermore, these solvent molecules and the complexes are engaged in an extensive weak hydrogen bonding network (C–H···F interactions; not shown in the figure) reinforcing the cohesion of the crystal structure.

Fig. 2 shows the UV–Vis spectrum of a solution of μ-O(FeTPFPP)$_2$ in methanol, which is essentially identical to those obtained for other similar μ-oxodimeric iron(III) porphyrins [23,40]. Four prominent absorption bands dominate the spectra: a broad band appears at 354 nm, a Soret band at 404 nm, two Q bands at 472 and 585 nm, consistent with the presence of the dimeric complex.

Table 2
Selected bond distances and angles of the Fe(III) coordination centre in the complex [μ-O(FeTPFPP)$_2$].

Distance (Å)		Angles (°)	
Fe1–N1	2.090(3)	N1–Fe1–N2	86.09(11)
Fe1–N2	2.103(3)	N1–Fe1–N3	148.91(11)
Fe1–N3	2.085(3)	N1–Fe1–N4	86.10(11)
Fe1–N4	2.095(3)	N1–Fe1–O1	105.93(12)
Fe1–O1	1.7730(5)	N2–Fe1–N3	86.17(11)
		N2–Fe1–N4	150.67(11)
		N2–Fe1–O1	105.95(9)
		N3–Fe1–N4	86.08(11)
		N3–Fe1–O1	105.15(12)
		N4–Fe1–O1	103.38(9)

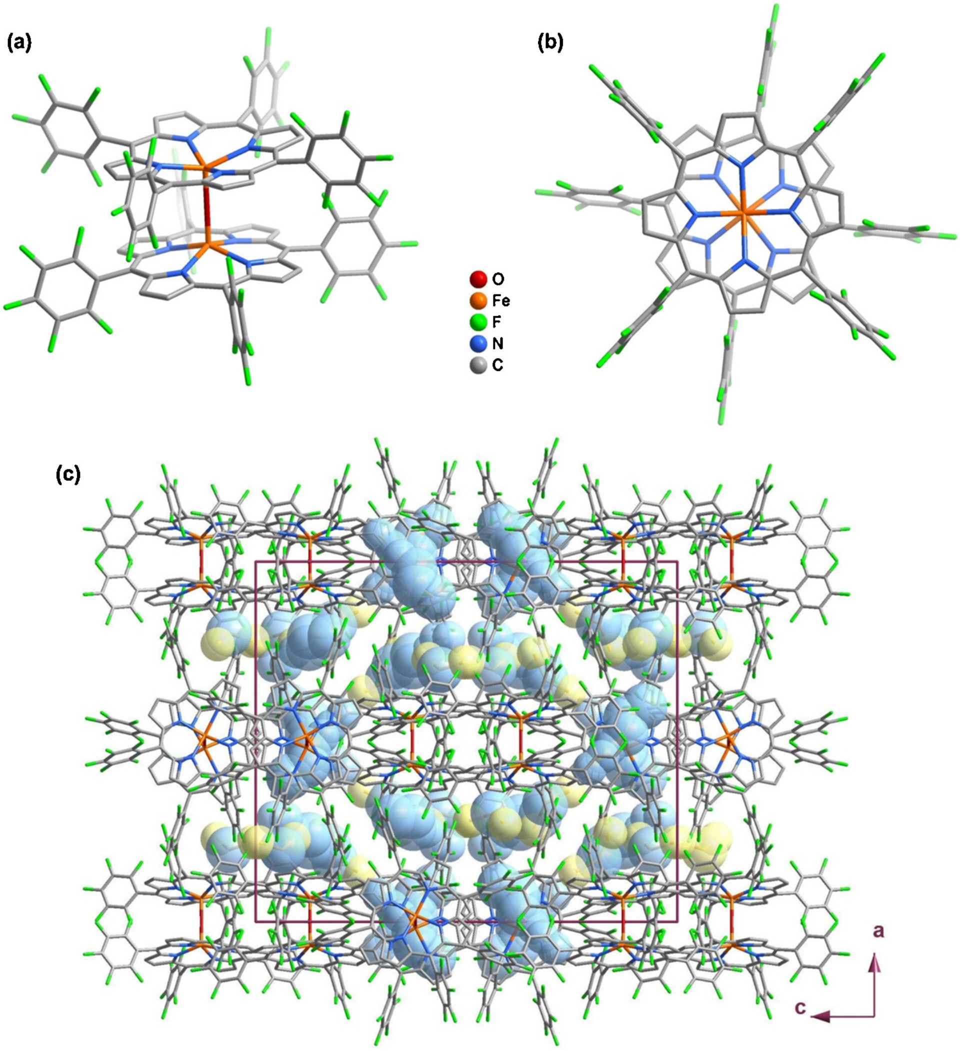

Fig. 1. Side (a) and top (b) views of the porphyrin complex [μ-O(FeTPFPP)$_2$], and the crystal packing (c) visualized in the [0 1 0] direction of the unit cell with the solvent molecules represented in the space-filling model. The hydrogen atoms were omitted for clarity reasons.

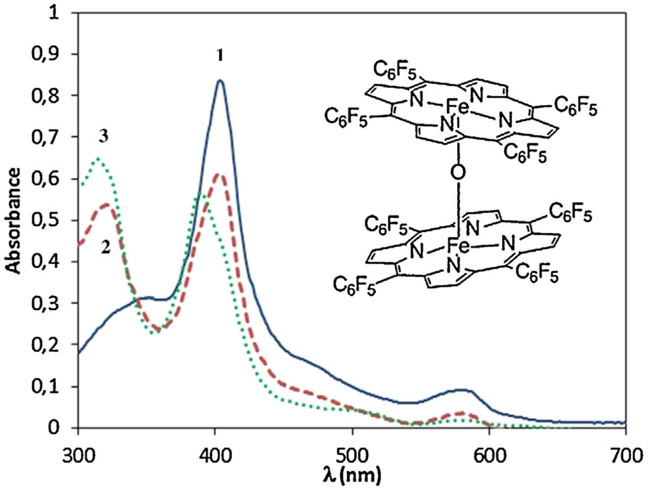

Fig. 2. In situ UV–Vis spectra of μ-O(FeTPFPP)$_2$ (1 μmol) in 0.75 mL of methanol (1, solid line), and immediately after the oxidative desulfurization cycles (2 for the first cycle and 3 for the second cycle) performed using a biphasic system multicomponent oil/MeOH as extraction solvent (1:1) and 2000 ppm (50 μmol, 5 μL) of H_2O_2 oxidant at room temperature. Consecutive ODS cycles were performed by adding the fresh multicomponent oil and an additional aliquot of 5 μL of H_2O_2 to the extraction phase containing the homogeneous porphyrin catalyst.

ESI-MS of μ-O(FeTPFPP)$_2$ dissolved in methanol confirmed the presence of the dimeric porphyrin species in solution, supporting the spectrophotometric and crystallographic data. The MH^+ ion of μ-O(FeTPFPP)$_2$ was observed at *m*/*z* 2072.957 with a resolution (FWHM) of 14701 and an associated mass error of −0.6 ppm. The high resolution mass determination together with the isotopic pattern observed allow to unequivocally assigning the chemical composition of the ion. Charge balance requires μ-O(FeTPFPP)$_2$ to be a neutral species with both iron centers in the Fe(III) oxidation state, an information confirmed by the absence of counter ions in the crystalline structure. Molecular ion fragmentation by higher-energy C-trap dissociation (HCD) retrieved the monomeric [FeTPFPP]$^+$ ion (*m*/*z* = 1027.969), providing supplementary evidence for the dimeric nature of the species.

3.2. Catalytic oxidative desulfurization studies

The μ-O(FeTPFPP)$_2$ porphyrin was applied as catalyst for the oxidative desulfurization (ODS) of a multicomponent oil containing the most representative refractory sulfur compounds in fuels: dibenzothiophene (DBT, i in Scheme 1), 1-benzothiophene (1-BT, ii) and 4,6-dimethyldibenzothiophene (4,6-DMDBT, iii). This model oil was prepared by dissolving each sulfur compound in n-octane to form solutions of approximately 500 ppm of sulfur from each

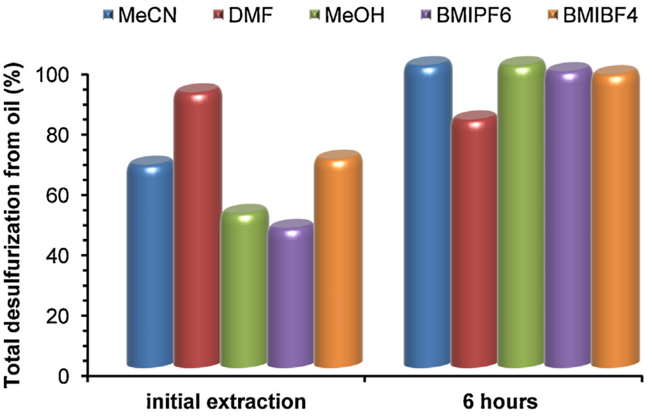

Fig. 3. Desulfurization data from the multicomponent oil (DBT + 1-BT + 4,6-DMDBT in *n*-octane, 0.75 mL) using different extraction solvents (0.75 mL), in the presence of dimeric μ-O(FeTPFPP)$_2$ porphyrin (1 μmol), 2000 ppm (50 μmol, 5 μL) of H_2O_2 at room temperature.

substrate. All the ODS experiments were performed in a biphasic system with equal volume of the model oil and an immiscible extracting organic solvent. The dimeric porphyrin showed to be a suitable homogeneous catalyst for the ODS technology since it was easily immobilized in different extracting organic solvents and no vestigial amount of it was found in the model oil representative of fuel.

Initially, an optimization of experimental parameters was performed, mainly for the nature of the extraction solvent, temperature reaction and oxidant H_2O_2 amount. In a typical experiment, the catalyst is initially dissolved in the extraction solvent and afterwards the model oil is added. The ODS processes studied consist of two main steps, the first corresponds to the initial extraction of the sulfur contents from the model oil to the extraction solvent only by stirring the two phases for 10 min, and the second is formed by the catalytic stage. This last catalytic step is started by the addition of the oxidant in order to convert the sulfur compounds into sulfones and sulfoxides, which are easily immobilized in the extraction solvent phase. In fact, the decrease of the non oxidised sulfur-compounds in the extracting phase causes a continuous transfer of these compounds from the oil phase to the extracting phase. ODS experiments in the absence of dimeric μ-O(FeTPFPP)$_2$ porphyrin were performed for the different studied conditions; however, negligible oxidative desulfurization was observed during the catalytic step.

The influence of the solvent extraction was investigated for the ODS process performed at room temperature and using 2000 ppm or 0.06 M (50 μmol, 5 μL) of H_2O_2. Different organic solvents were tested (MeOH, MeCN, DMF), as well as two different ionic liquids (ILs) having the same cation and two different anions: 1-butyl-3-methylimidazolium hexafluorophosphate (BMIPF$_6$) and tetrafluoroborate (BMIBF$_4$). The efficiency of these ILs as extraction solvents has been already reported in the literature for desulfurization systems in the absence of catalyst [41,42] or using oxometalates as catalyts [9,43,44]. The main difference between these two ILs corresponds to the miscibility with the oxidant, since BMIBF$_4$ dissolves the aqueous H_2O_2 and the BMIPF$_6$ forms a triphasic system because it is more hydrophobic and immiscible with H_2O_2. Fig. 3 compares the desulfurization of multicomponent oil after 10 min stirring before the addition of the oxidant (initial extraction step) and after 6 h of the catalytic stage. It can be observed that the largest desulfurization occurs during the initial extraction step. When DMF was used, a largest initial extraction was observed (91% of sulfur compounds are transferred from model oil to DMF, after 10 min of stirring at room temperature), followed by MeCN (67%) and the ionic liquid BMIBF$_4$ (69%). Between the different sulfur compounds, similar extraction was found for DBT, 1-BT and 4,6-DMDBT, when DMF was used. However, in the presence of BMIBF$_4$ and MeCN lower extraction was observed for 4,6-DMDBT (detailed amounts for each sulfur compound are given in Table S1 in ESI). In accordance with other previous desulfurization studies, the refractory no-oxidized sulfur compounds are more soluble in higher polar organic solvents such as in DMF than in MeCN and methanol [7].

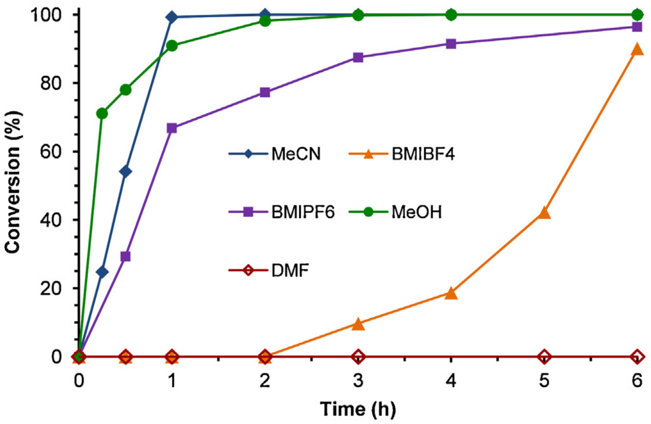

Fig. 4. Kinetic profile for the oxidation of sulfur refractory compounds catalyzed by μ-O(FeTPFPP)$_2$ porphyrin (1 μmol) using different biphasic systems formed by multicomponent sulfur oil (DBT + 1-BT + 4.6-DMDBT in *n*-octane, 0.75 mL) and several polar solvents (0.75 mL). Reactions performed at room temperature and the time 0 h correspond to the addition of H_2O_2 (50 μmol, 5 μL) to the ODS system.

After the large extraction of refractory sulfur enhanced during the first 10 min of stirring, further desulfurization is achieved during the catalytic oxidative stage initiated after the addition of the oxidant. It is important to note that the oxidation of the sulfur compounds may occur in the solvent extraction phase, since neither the catalyst nor the oxidant are present in the oil phase and also because no oxidized products were detected in the oil phase. The decrease of the refractory benzothiophenes derivatives in the solvent extraction phase caused by their oxidation promotes a continuous transfer of these sulfur compounds from the oil phase to the solvent extraction phase. Fig. 4 presents the kinetic profile of the homogeneous μ-O(FeTPFPP)$_2$ catalyst during the catalytic stage of the ODS process in the presence of different extraction solvents. It is important to note that the conversion data displayed in Fig. 4 correspond to the sulfur content (DBT, 1-BT and 4,6-DMDBT) present in the model oil phase during the catalytic stage. It can be observed that the best solvent during the initial extraction step, i.e. DMF, does not promoted any catalytic oxidation of the sulfur components into sulfoxides and/or sulfones. In fact, in the presence of DMF the desulfurization achieved after the initial extraction was even slightly higher than after the 6 h of catalytic stage. This behavior was also observed before and may be caused by the addition of the aqueous oxidant in the extraction solvent phase [7]. Comparing the different kinetic profiles in Fig. 4 it is possible to conclude that the best extraction solvents to achieve a total desulfurization in shorter reaction time are MeCN and MeOH. Reasonable desulfurization efficiency was found using the ionic liquid BMIPF$_6$; however in the presence of MeOH and MeCN a complete desulfurization of the multicomponent oil was obtained after 2 h, while in the presence of BMIPF$_6$ 219 ppm of sulfur was still present in the oil. After the 6 h, the presence of sulfur in the multicomponent oil was also 34 ppm using BMIPF$_6$, 55 ppm using BMIBF$_4$ and 319 ppm using DMF. Therefore, the elected solvents for the ODS process catalyzed by μ-O(FeTPFPP)$_2$ porphyrin were MeOH and MeCN.

The influence of the oxidant amount was also investigated for the ODS system of multicomponent oil/MeOH at room

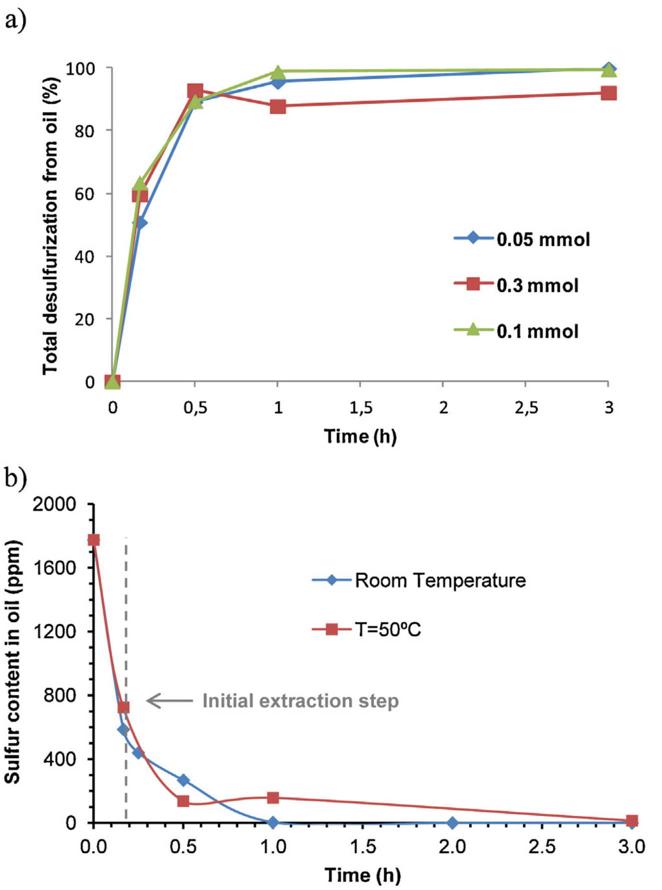

Fig. 5. (a) Desulfurization profile of a multicomponent oil (DBT + 1-BT + 4.6-DMDBT in *n*-octane, 0.75 mL), using a biphasic systems oil/MeOH (1:1) at room temperature, catalyzed by μ-O(FeTPFPP)$_2$ porphyrin (1 μmol), using different amounts of H_2O_2 oxidant (5, 10, 30 μL). (b) desulfurization process at room temperature and at 50 °C, using the multicomponent oil/MeOH (1:1) system, catalyzed by μ-O(FeTPFPP)$_2$ porphyrin (1 μmol) in the presence of H_2O_2 (50 μmol, 5 μL).

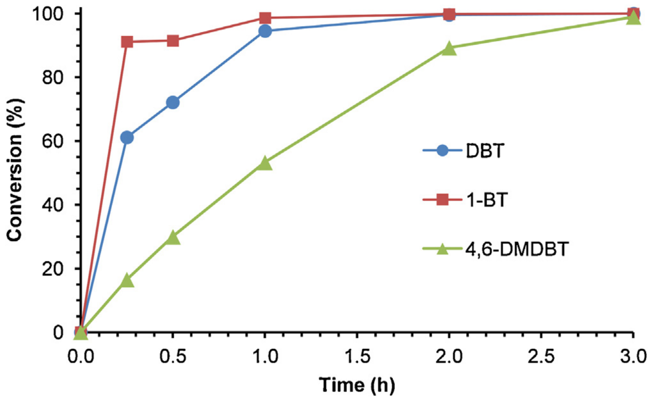

Fig. 6. Kinetic profile for the oxidation of the various sulfur refractory compounds in the model oil (500 ppm of each sulfur compound in *n*-octane) catalyzed by μ-O(FeTPFPP)$_2$ porphyrin (1 μmol), at room temperature, using the biphasic system oil/MeOH as extraction solvent (1:1). The time 0 h correspond to the addition of H_2O_2 (50 μmol, 5 μL) to the ODS system.

temperature. The desulfurization of the same model oil was tested using 2000, 4000 and 12000 ppm of H_2O_2 (0.05, 0.1 and 0.3 mmol, respectively, in 0.75 mL of extraction solvent). Fig. 5a shows that similar efficiency was found using 2000 and 4000 ppm of oxidant and, when its amount was increased to 12,000 ppm, lower desulfurization was achieved, mainly after the first hour of reaction. This decrease of desulfurization must be due to some catalyst decomposition when it is exposed to the presence of a high amount of oxidant.

A comparison of the efficiency of μ-O(FeTPFPP)$_2$ catalyst for the desulfurization of the multicomponent oil was performed at room temperature (20–23 °C) and at 50 °C, using MeOH as solvent extraction and H_2O_2 (2000 ppm, 50 μmol) as oxidant. Fig. 5b presents that the total desulfurization from oil at room temperature and at 50 °C is very similar for the initial extraction step and during the first minutes of the catalytic stage. However, after 1 h almost complete desulfurization was achieved at room temperature, while at 50 °C the same result was only obtained after 3 h. These results indicate that the best conditions to achieved the highest efficiency of μ-O(FeTPFPP)$_2$ for the ODS processes is using a small amount of H_2O_2 oxidant at room temperature. Probably, these are the conditions that allow the porphyrin catalyst to operate without decomposition and promote an efficient interaction between catalyst, sulfur compound and oxidant.

Fig. 6 display the kinetic profile for the oxidation of each refractory sulfur compound present in the model oil (DBT, 1-BT and 4,6-DMDBT), using MeOH as solvent extraction, 2000 ppm of H_2O_2 at room temperature. After the first hour the extraction of DBT and 1-BT is practically completed, remaining only 7 ppm of sulfur corresponding to 1-BT (95% of conversion) and 10 ppm of sulfur attributed to DBT (98% of conversion) in the model oil. However, the 4,6-DMDBT is more difficult of removing from the oil because the efficiency of the Fe^{III} porphyrin catalyst is lower to oxidize this sulfur compound. It is well reported in the literature that the reactivity of the studied refractory sulfur compounds decreases in the order of DBT > 4,6-DMDBT > 1-BT [45–51]. The lowest reactivity of 1-BT is attributed to the significant lower electron density on the sulfur atom of 1-BT. Between DBT and 4,6-DMDBT, the difference of electron density on the sulfur atom is very small [52]. However, previous studies using Fe^{III} porphyrin as catalyst to oxidize DBT and 4,6-DMDBT in the presence of O_2 also demonstrate that 4,6-DMDBT is more difficult to oxidize than DBT due to the higher interaction of this sulfur compound with the porphyrin catalyst rather than with the oxidant [17]. Post-catalysis ESI-MS (Fig. 7) confirmed this interaction, revealing the formation of an adduct between 4,6-DMDBT sulfoxide and a FeTPFPP monomer at *m*/*z* value 1256.044 ($\Delta m < 5$ ppm). This was the only FeTPFPP adduct formed either with reagents or reaction products, which exposes the specific ability of 4,6-DMDBT sulfoxide to form a stable interaction with FeTPFPP.

Only a few examples can be found in the literature reporting the application of metalloporphyrins as catalysts for the oxidation of DBT, 1-BT or 4,6-DMDBT. Zhou et al. reported the oxidation of DBT and 4,6-DMDBT using a Fe^{III} porphyrin as catalyst. The total oxidation of these substrates was achieved after 3 h; however, a temperature of 120 °C was needed [17]. The oxidation of 1-BT and DBT in MeCN and hexane media were studied recently at room temperature using Mn porphyrins as catalyst and H_2O_2 as oxidant [53]. Also in this study the oxidation of 1-BT was faster than the oxidation of DBT and almost complete conversion into the corresponding sulfones was obtained after 1.5 and 2 h when ammonium acetate was used as co-catalyst. It is important to note that the faster oxidation of 1-BT using Mn porphyrins is consistent with the faster kinetic profile obtained in this study using a Fe porphyrin. In fact, the catalytic efficiency of different porphyrins having different metal ions to oxidize 1-BT is similar. This data may suggest that the mechanism should not be trivial and must be related to an intrinsic property of porphyrins.

The reusability of the ODS system multicomponent oil/MeOH catalyzed by the μ-O(FeTPFPP)$_2$ porphyrin, using 2000 ppm (50 μmol of H_2O_2) oxidant was studied. After the ODS process, the sulfur-free oil phase was removed from the system, remaining the MeOH phase that immobilize the porphyrin catalyst. An

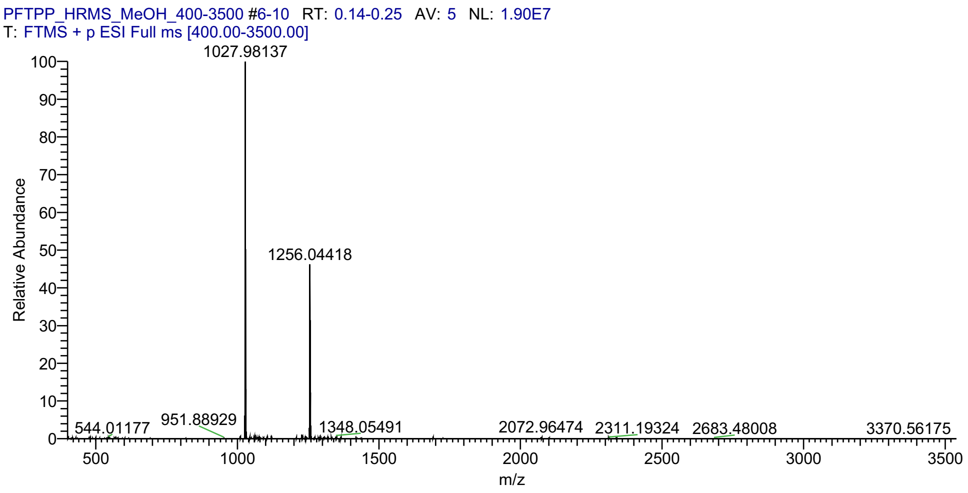

Fig. 7. High resolution electrospray ionisation mass spectra obtained after the oxidative desulfurization process of a multicomponent oil (DBT + 1-BT + 4,6-DMDBT in *n*-octane, 0.75 mL) catalyzed by the dimeric μ-O(FeTPFPP)$_2$ porphyrin (1 μmol), using the biphasic system oil/MeOH as extraction solvent (1:1), 2000 ppm (50 μmol, 5 μL) of H_2O_2 at room temperature.

additional 50 μmol of H_2O_2 and a fresh portion of model oil were added to the systems and a new desulfurization process occurred. This reusability process was repeated for various consecutive ODS cycles and the results are presented in Fig. 8. A slight decrease in the desulfurization efficiency may be mentioned from the first to the consecutive cycles, mainly during the first 3 h. The conversion data displayed in Fig. 7 for each sulfur compound demonstrates that this small decrease in the efficiency of desulfurization is probably due to a reduction in the activity of the catalyst towards 4,6-DMDBT oxidation, since the catalytic oxidation of DBT and 1-BT was maintained between ODS cycles. It is also important to mention that after the first ODS cycle, the sulfones products of the sulfur refractory compounds precipitate in the extraction phase (MeOH) and could be removed from the ODS system by simple filtration.

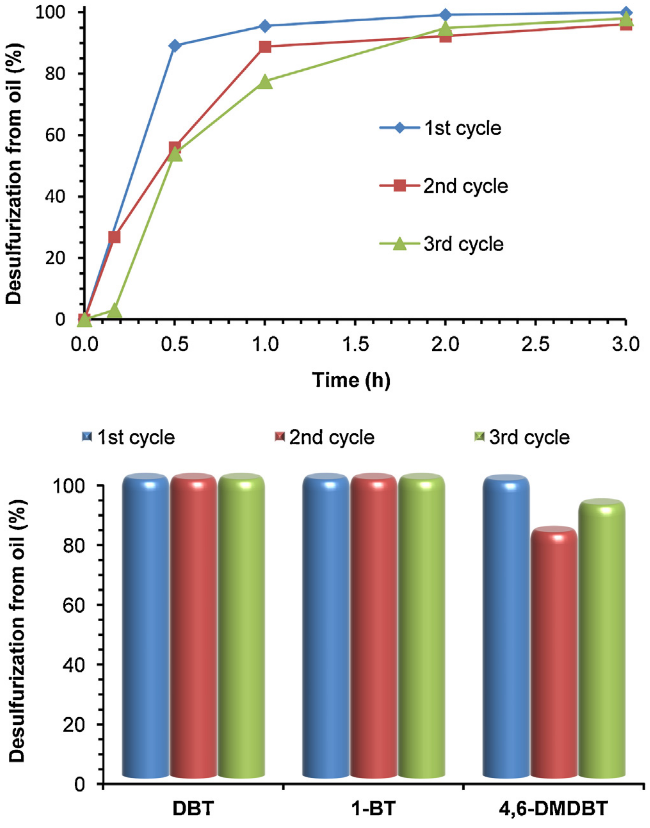

Fig. 8. Kinetic profile (on top) for three consecutive desulfurization cycles of a multicomponent oil (DBT + 1-BT + 4.6-DMDBT in *n*-octane, 0.75 mL) catalyzed by μ-O(FeTPFPP)$_2$ porphyrin (1 μmol) at room temperature, using a biphasic system oil/MeOH as extraction solvent (1:1) and 2000 ppm (50 μmol, 5 μL) of H_2O_2 oxidant. On bottom, conversion data obtained for each sulfur refractory component from muticomponent oil after 3 h.

The stability of μ-O(FeTPFPP)$_2$ porphyrin after catalytic use was investigated performing the UV–Vis spectrum of the extraction solvent at the end of desulfurization cycles (Fig. 2). Some variations are observed in the spectra after catalytic use. The disappearing of the broad band at 354 nm suggests the cleavage of the Fe-O bond of the μ-oxo dimer with the concomitant formation of two monomeric porphyrins and a shift of the Soret band from 404 nm to 388 nm. This behavior was already observed before by Cunningham and coworkers, after the treatment of Fe(III) TPFPP with H_2O_2, which it is attributed to the formation of the Fe(III)-H_2O_2 complex [54].

4. Conclusions

The μ-oxo-bridged Fe(III) complex of *meso*-tetrakis(pentafluorophenyl)porphyrin (μ-O(FeTPFPP)$_2$) was successfully prepared and characterized by UV/Vis spectroscopy, mass spectrometry and single-crystal X-ray diffraction. The dimeric metalloporphyrin was applied as efficient catalyst for the desulfurization of a model oil containing various benzothiophenes derivatives as the most sulfur refractory compounds present in fuels. A biphasic system formed by the model oil and a polar organic solvent containing the metalloporphyrin was used. An optimization of different parameters was preformed, namely the nature of the extraction solvent, amount of H_2O_2 as oxidant and reaction temperature. Acetonitrile and methanol presented to be the best extraction solvents to achieve a total desulfurization after 2 h and the best conditions to reach the highest catalytic efficiency of μ-O(FeTPFPP)$_2$ is in the presence of a small amount of oxidant (2000 ppm and S/Oxid ratio of 0.75) at room temperature. Furthermore, the efficiency of the catalyst for the desulfurization of each sulfur compounds was analyzed and surprisingly a remarkable performance was found for the extraction of 1-BT and DBT from the model oil caused by the effective activity of the porphyrin to catalyze their oxidation. The lower efficiency for 4,6-DMDBT was investigated by ESI-MS and this is probably caused by the formation of an adduct between the 4,6-DMDBT and the catalyst. For the desulfurization system using methanol as extraction solvent, the reusability of the homogenous catalyst was performed without appreciable loss of activity between three consecutive cycles.

Actually, we are exploring other porphyrins with distinct substituent groups and metal centers to better understand the involvement of these catalysts in the desulfurization process.

Acknowledgments

This work was supported by Fundação para a Ciência e a Tecnologia (FCT, Portugal), European Union, QREN, FEDER and COMPETE, projects NORTE-07-0162-FEDER-000048, NORTE-07-0124-FEDER-000066/67, PEst-C/EQB/LA0006/2011 and the R&D project PTDC/EQU-EQU/121677/2010. The NMR spectrometers are part of the National NMR Network and were purchased in the framework of the National Programme for Scientific Re-equipment, contract REDE/1517/RMN/2005, with funds from POCI 2010 (FEDER) and Fundação para a Ciência e a Tecnologia (FCT).

Appendix A. Supplementary data

Supplementary material related to this article can be found, in the online version, at http://dx.doi.org/10.1016/j.apcata.2014.04.002.

References

[1] A. Seeberger, A. Jess, Green Chem. 12 (2010) 602–608.
[2] X. Zhou, S. Lv, H. Wang, X. Wang, J. Liu, Appl. Cat. A - Gen. 396 (2011) 101–106.
[3] V.C. Srivastava, RSC Adv. 2 (2012) 759–783.
[4] Z. Ismagilov, S. Yashnik, M. Kerzhentsev, V. Parmon, A. Bourane, F.M. Al-Shahrani, A.A. Hajji, O.R. Koseoglu, Catal. Rev.-Sci. Eng. 53 (2011) 199–255.
[5] X. Chen, D. Song, C. Asumana, G. Yu, J. Mol. Cat. A - Chem. 359 (2012) 8–13.
[6] B. Pawelec, R.M. Navarro, J.M. Campos-Martin, J.L.G. Fierro, Catal. Sci. Technol. 1 (2011) 23–42.
[7] S. Ribeiro, C.M. Granadeiro, P. Silva, F.A. Almeida Paz, F.F. de Biani, L. Cunha-Silva, S.S. Balula, Catal. Sci. Technol. 3 (2013) 2404–2414.
[8] S. Ribeiro, A.D.S. Barbosa, A.C. Gomes, M. Pillinger, I.S. Gonçalves, L. Cunha-Silva, S.S. Balula, Fuel Proc. Tech. 116 (2013) 350–357.
[9] J.H. Xu, S. Zhao, W. Chen, M. Wang, Y.F. Song, Chem. Eur. J. 18 (2012) 4775–4781.
[10] P. Jourdain, F. Philippart, R. Dumeunier, I.E. Marko, Tetrahedron Lett. 50 (2009) 3366–3370.
[11] A. Alizadeh, M.M. Khodaei, E. Nazari, Tetrahedron Lett. 48 (2007) 6805–6808.
[12] Q.H. Xia, H.Q. Ge, C.P. Ye, Z.M. Liu, K.X. Su, Chem. Rev. 105 (2005) 1603–1662.
[13] C.M. Drain, A. Varotto, I. Radivojevic, Chem. Rev. 109 (2009) 1630–1658.
[14] S.M. Chen, S.W. Chiu, J. Mol. Cat. A - Chem. 166 (2001) 243–253.
[15] S. Evans, J.R.L. Smith, J. Chem. Soc. - Perkin Trans. (2001) 174–180.
[16] S.M. Chen, J. Mol. Cat. A - Chem. 138 (1999) 1–13.
[17] X.R. Zhou, S. Lv, H. Wang, X.N. Wang, J.H. Liu, Appl. Cat. A - Gen. 396 (2011) 101–106.
[18] S.M.G. Pires, M.M.Q. Simoes, I. Santos, S.L.H. Rebelo, M.M. Pereira, M. Neves, J.A.S. Cavaleiro, Appl. Cat. A - Gen. 439 (2012) 51–56.
[19] A. Rezaeifard, M. Jafarpour, H. Raissi, E. Ghiamati, A. Tootoonchi, Polyhedron 30 (2011) 592–598.
[20] C.-C. Guo, X.-Q. Liu, Z.-P. Li, D.-C. Guo, Appl. Cat. A - Gen. 230 (2002) 53–60.
[21] C.-C. Guo, X.-Q. Liu, Y. Liu, Q. Liu, M.-F. Chu, X.-B. Zhang, J. Mol. Cat. A - Chem. 192 (2003) 289–294.
[22] C. Guo, Q. Peng, Q. Liu, G. Jiang, J. Mol. Cat. A - Chem. 192 (2003) 295–302.
[23] X.-T. Zhou, Q.-H. Tang, H.-B. Ji, Tetrahedron Lett. 50 (2009) 6601–6605.
[24] A.M.d.A.R. Gonsalves, J.M.T.B. Varejão, M.M. Pereira, J. Heterocyclic Chem. 28 (1991) 635–640.
[25] T. Kottke, D. Stalke, J. App. Cryst. 26 (1993) 615–619.
[26] APEX2, Data Collection Software Version 2.1-RC13, Bruker AXS, Delft, The Netherlands (2006).
[27] Cryopad, Remote monitoring and control, Version 1.451, Oxford Cryosystems, Oxford, United Kingdom (2006).
[28] SAINT+, Data Integration Engine v. 7.23a ©, (1997–2005) Bruker AXS, Madison, Wisconsin, USA.
[29] G.M. Sheldrick, SADABS v.2.01, Bruker/Siemens Area Detector Absorption Correction Program, Bruker AXS, Madison, Wisconsin, USA (1998).
[30] G.M. Sheldrick, SHELXS-97, Program for Crystal Structure Solution, University of Göttingen (1997).
[31] G.M. Sheldrick, Acta Cryst. A 64 (2008) 112–122.
[32] G.M. Sheldrick, SHELXL-97, Program for Crystal Structure Refinement, University of Göttingen (1997).
[33] A. Gold, K. Jayaraj, P. Doppelt, J. Fischer, R. Weiss, Inorg. Chim. Acta 150 (1988) 177–181.
[34] T.D. Ju, R.A. Ghiladi, D.-H. Lee, G.P.F. van Strijdonck, A.S. Woods, R.J. Cotter, V.G. Young, K.D. Karlin, Inorg. Chem. 38 (1999) 2244–2245.
[35] T. Hayashi, Y. Nakashima, K. Ito, T. Ikegami, I. Aritome, K. Aoyagi, T. Ando, Y. Hisaeda, Inorg. Chem. 42 (2003) 7345–7347.
[36] K.A. de Villiers, H.M. Marques, T.J. Egan, J. Inorg. Biochem. 102 (2008) 1660–1667.
[37] S.M. Gorun, J.W. Rathke, M.J. Chen, Dalton Trans. (2009) 1095–1097.
[38] N. Xu, D.R. Powell, G.B. Richter-Addo, Angew. Chem. Int. Ed. 50 (2011) 9694–9696.
[39] T. Straasø, S. Kapishnikov, K. Kato, M. Takata, J. Als-Nielsen, L. Leiserowitz, Cryst. Growth Des. 11 (2011) 3342–3350.
[40] S.K. Ghosh, R. Patra, S.P. Rath, Inorg. Chim. Acta 363 (2010) 2791–2799.
[41] X.M. Liu, G.H. Zhou, X.P. Zhang, S.J. Zhang, Aiche J. 56 (2010) 2983–2996.
[42] B. Zhang, M.D. Zhou, M. Cokoja, J. Mink, S.L. Zang, F.E. Kuhn, RSC Adv. 2 (2012) 8416–8420.
[43] H.Y. Lu, W.Z. Ren, H.Y. Wang, Y. Wang, W. Chen, Z.H. Suo, Appl. Cat. A. - Gen. 453 (2013) 376–382.
[44] H.M. Li, X. Jiang, W.H. Zhu, J.D. Lu, H.M. Shu, Y.S. Yan, Ind. Eng. Chem. Res. 48 (2009) 9034–9039.
[45] C. Komintarachat, W. Trakarnpruk, Ind. Eng. Chem. Res. 45 (2006) 1853–1856.
[46] M. Te, C. Fairbridge, Z. Ring, Appl. Cat. A - Gen. 219 (2001) 267–280.
[47] X. Jiang, H.M. Li, W.S. Zhu, L.N. He, H.M. Shu, J.D. Lu, Fuel 88 (2009) 431–436.
[48] M.A. Rezvani, A.F. Shojaie, M.H. Loghmani, Cat. Comm. 25 (2012) 36–40.
[49] W. Zhu, W. Huang, H. Li, M. Zhang, W. Jiang, G. Chen, C. Han, Fuel Proc. Tech. 92 (2011) 1842–1848.
[50] J. Xu, S. Zhao, W. Chen, M. Wang, Y.-F. Song, Chem. Eur. J. 18 (2012) 4775–4781.
[51] W. Trakarnpruk, K. Rujiraworawut, Fuel Proc. Tech. 90 (2009) 411–414.
[52] S. Otsuki, T. Nonaka, N. Takashima, W.H. Qian, A. Ishihara, T. Imai, T. Kabe, Energy Fuels 14 (2000) 1232–1239.
[53] S.M.G. Pires, M.M.Q. Simoes, I.C.M.S. Santos, S.L.H. Rebelo, M.M. Pereira, M.G.P.M.S. Neves, J.A.S. Cavaleiro, Appl. Cat. A - Gen. 439 (2012) 51–56.
[54] I.D. Cunningham, A. Basaleh, H.A. Gazzaz, Dalton Trans. 41 (2012) 9158–9160.